DESIGN AND ANALYSIS OF OFFSET SLIDER-CRANK WITH TRANSLATING ROLLER-FOLLOWER

Jung-Fa Hsieh
Jung-Fa Hsieh, Far East University, Tainan, 74448, Taiwan
E-mail: seznof@cc.feu.edu.tw

Received February 2011, Accepted May 2011
No. 11-CSME-12, E.I.C. Accession 3252

ABSTRACT

This paper presents a systematic methodology for the design and analysis of an offset slider-crank mechanism with a translating roller-follower. In the proposed approach, a generic kinematic model of the offset slider-crank and roller-follower is constructed using a homogenous coordinate transformation method and the slider cam profile are then derived using conjugate surface theory. The pressure angle and principal curvatures of the designed slider cam are analyzed based on the analytical expression of the cam profile. Finally, the NC data required to machine the slider cam are produced by equating the ability matrix of the 3-axis CNC machine tool with the desired tool location matrix.

Keywords: slider-crank; homogenous coordinate transformation; conjugate surface theory; principal curvature.

CONCEPTION ET ANALYSE D'UN MÉCANISME BIELLE-MANIVELLE À MOUVEMENT DÉCALÉ ET ROULEAU SUIVEUR EN TRANSLATION

RÉSUMÉ

L'article porte sur une méthode systématique pour la conception et l'analyse d'un mécanisme bielle-manivelle à mouvement décalé et rouleau suiveur en translation. Un modèle cinématique générique du mécanisme bielle-manivelle à mouvement décalé et rouleau suiveur est élaboré en utilisant une méthode de transformation coordonnée homogène, et le profil du coulisseau à came est dérivé en utilisant la théorie des surfaces conjuguées. L'angle de pression et les courbures principales du coulisseau à came sont analysés sur la base de l'expression analytique du profil de la came. Finalement, les données CN requises pour fabriquer le coulisseau à came sont produites en testant l'efficacité de la matrice de la machine-outil CNC à trois axes à l'emplacement désiré.

Mots-clés : mécanisme bielle-manivelle; transformation coordonnée homogène; théorie des surfaces conjuguées; courbure principale.

1. INTRODUCTION

Cam mechanisms are used in many modern machines, including weaving looms, precision measurement instruments, automatic machine tools, automobile engines, and so on. In conventional cam systems with a translating roller-follower mechanism, the cam is installed directly on the main shaft. However, for reasons of space constraints, it is sometimes necessary to install the cam mechanism remotely from the driving shaft. For example, in [1], the authors considered the case where a cutting tool used to form nuts could not be driven directly by the main shaft due to space restrictions, but was attached instead to a translating roller-follower, driven in turn by a slider-crank.

The problem of cam profile synthesis for cam mechanisms with translating roller-followers has been discussed in many books and studies [2–6]. However, in most cases, the literature considers a conventional cam type mechanism in which the cam is built into the main shaft and the rotation of the shaft causes a direct translation of the follower. By contrast, the literature contains little information regarding the profile synthesis of slider crank systems in which the rotation of the crank drives a remote slider cam, which in turn drives a translating follower. Wu, et al [1] presented a geometric approach based on instant velocity center theory for synthesizing the profile of a slider-crank with a translating follower. However, the problem of converting the designed profile into a set of NC machining instructions was not considered. Accordingly, the current study presents a systematic methodology for both the design and the fabrication of an offset slider-crank mechanism with a translating roller-follower. The proposed methodology comprises four basic steps: (1) establish a kinematic model of the offset slider-crank and roller-follower, (2) perform a kinematic analysis of the slider-crank and follower and derive the slider cam profile, (3) analyze the pressure angle and principal curvatures of the designed slider cam, and (4) obtain the ability matrix (the position and orientation of the spindle with respect to the table frame) of the 3-axis CNC machine tool and the desired tool location matrix (the position and orientation of the cutter) and generate the NC code required to machine the designed slider cam. The validity of the proposed approach is demonstrated by machining a slider cam on a 3-axis vertical CNC machine tool.

In the analysis performed in this study, the point vector $a_x\boldsymbol{i}+a_y\boldsymbol{j}+a_z\boldsymbol{k}$ is written in the form of a column matrix ${}^{j}\boldsymbol{a}=[\mathrm{a_x}\ \mathrm{a_y}\ \mathrm{a_z}\ 1]^{\mathrm{T}}$, where the pre-superscript "j" of the leading symbol indicates that the vector is defined with respect to the coordinate frame $(\mathrm{xyz})_{\mathrm{j}}$. Furthermore, given a point ${}^{j}\boldsymbol{a}$, its transformation, ${}^{k}\boldsymbol{a}$, is represented by the matrix product ${}^{k}\boldsymbol{a}={}^{k}\boldsymbol{A}_{j}\,{}^{j}\boldsymbol{a}$, where ${}^{k}\boldsymbol{A}_{j}$ is a 4×4 matrix defining the position and orientation (referred to hereafter as "configuration") of frame $(\mathrm{xyz})_j$ with respect to frame $(\mathrm{xyz})_k$. Note that the same notation rules are applied to the unit directional vector, i.e. ${}^{j}\boldsymbol{n}=[\mathrm{n}_x\ \mathrm{n}_y\ \mathrm{n}_z\ 0]^{\mathrm{T}}$. Note also that for simplicity, if a vector is referred to the cam frame, i.e. $(\mathrm{xyz})_0$, the pre-superscript, "0", is omitted.

2. SLIDER CAM PROFILE

In using the Denavit-Hartenberg (D–H) notation to describe the kinematics of a mechanical system comprising a series of interconnected links, each link is assumed to have two actuated joints, i.e. i and $i+1$ [7]. To describe the kinematic relationship between the links, the following four parameters are required (see Fig. 1): (1) the common normal distance a_i between the axes of joints i and $i+1$; (2) the angle α_i between the axes of the two joints in a plane perpendicular to a_i; (3) the link offset b_i , i.e. the distance measured along axis z_{i-1} from 0_{i-1} (the origin of frame $(\mathrm{xyz})_{i-1}$) to the intersection of a_i and axis z_{i-1}; and (4) the link angle θ_i , i.e. the angle between x_{i-1}

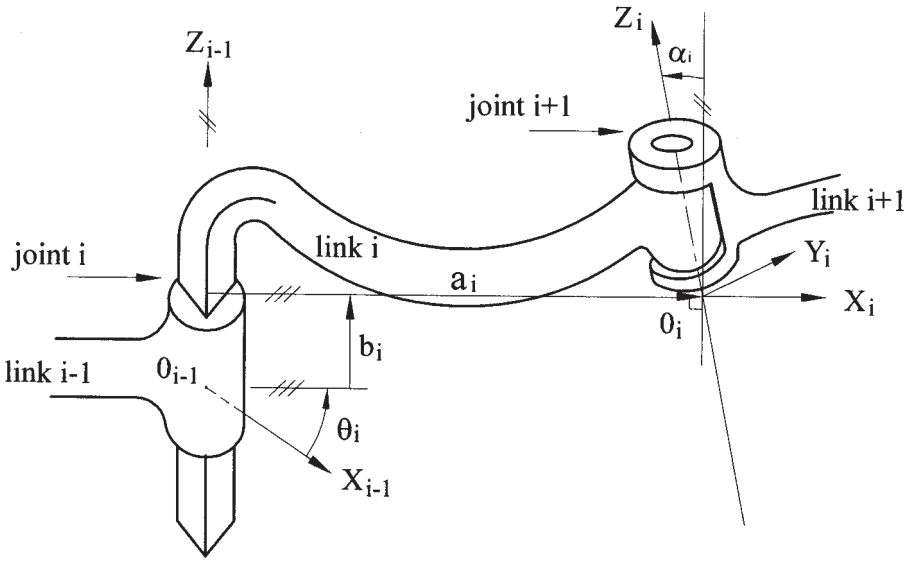

Fig. 1. The Denavit-Hartenberg parameters used for modelling the joints.

and x_i measured in a plane normal to z_{i-1}. The configuration of frame $(xyz)_i$ with respect to frame $(xyz)_{i-1}$ can be expressed as

$$
\begin{aligned}
{}^{i-1}\boldsymbol{A}_i &= \boldsymbol{Rot}(z,\theta_i)\,\boldsymbol{Trans}(0,0,b_i)\;\boldsymbol{Trans}(a_i,0,0)\;\boldsymbol{Rot}(x,\alpha_i) \\
&= \begin{bmatrix} C\theta_i & -S\theta_i C\alpha_i & S\theta_i S\alpha_i & a_i C\theta_i \\ S\theta_i & C\theta_i C\alpha_i & -C\theta_i S\alpha_i & a_i S\theta_i \\ 0 & S\alpha_i & C\alpha_i & b_i \\ 0 & 0 & 0 & 1 \end{bmatrix}
\end{aligned} \tag{1}
$$

where C and S denote COSINE and SINE, respectively.

Figure 2 illustrates the offset slider-crank with translating roller-follower considered in the present analysis. As shown, the crank rotates at a constant angular velocity of w_3, causing a reciprocating motion of the slider cam and a corresponding translation of the roller-follower. The major components of the slider crank mechanism include the crank link, the float link, the slider cam, the translating follower, and a fixed frame. In order to synthesize the cam profile, it is first necessary to number all of the links in the cam mechanism sequentially, starting with the slider cam (marked as "0" in Fig. 2) and ending with the translating roller-follower (marked as "4" in Fig. 2). Although the mechanism shown in Fig. 2 is a closed-loop mechanism, the designation "3" refers to the fixed frame rather than the slider since the D–H notation is invalid in the kinematic pair between the slider cam and the meshing element. Once the frames $(xyz)_i$ ($i=0,..4$) have been assigned to link i according to the D–H notation, the kinematic parameters can be tabulated, as shown in Table 1. The configuration of frame $(xyz)_4$ with respect to frame $(xyz)_0$ is given by

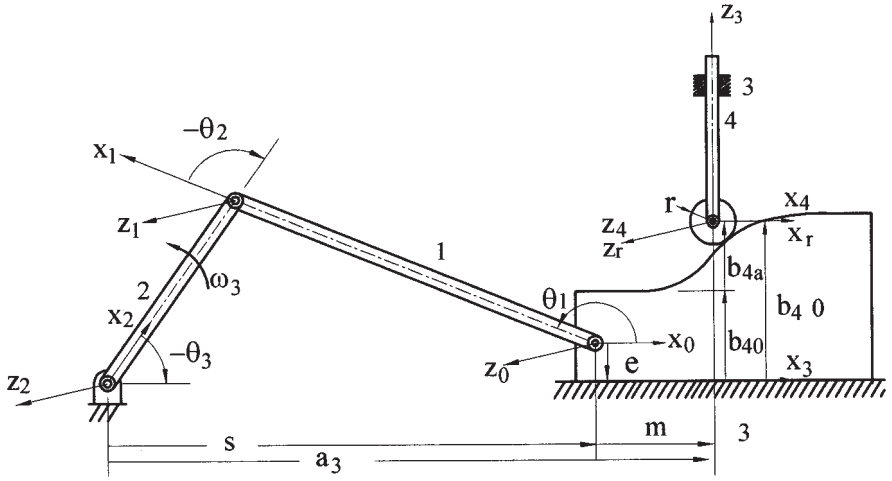

Fig. 2. Offset slider-crank mechanism with translating roller-follower.

$$ {}^{0}\mathbf{A}_4 = \prod_{i=1}^{4} {}^{i-1}\mathbf{A}_i = \begin{bmatrix} 1 & 0 & 0 & m \\ 0 & 1 & 0 & b_4 - e \\ 0 & 0 & 1 & 0 \\ 0 & 0 & 0 & 1 \end{bmatrix}. \tag{2} $$

Note that $b_4 = b_4(\theta_3)$ specifies the input-output relationship of the mechanism. In Fig. 2, the parameter b_{40} denotes the initial position (i.e. lower dwell position) of the roller-follower, while b_{4a} is the displacement of the roller-follower in the vertical direction. The configuration of frame $(xyz)_r$ (embedded in the roller) with respect to frame $(xyz)_4$ can be expressed as

$$ {}^{4}\mathbf{A}_r = \begin{bmatrix} 1 & 0 & 0 & 0 \\ 0 & 1 & 0 & 0 \\ 0 & 0 & 1 & 0 \\ 0 & 0 & 0 & 1 \end{bmatrix}. \tag{3} $$

Meanwhile, the configuration of the roller frame $(xyz)_r$ with respect to frame $(xyz)_0$ can be expressed as

$$ {}^{0}\mathbf{A}_r = {}^{0}\mathbf{A}_4 \, {}^{4}\mathbf{A}_r = \begin{bmatrix} 1 & 0 & 0 & m \\ 0 & 1 & 0 & b_4 - e \\ 0 & 0 & 1 & 0 \\ 0 & 0 & 0 & 1 \end{bmatrix}. \tag{4} $$

In Fig. 3, the surface equation, ${}^{r}\boldsymbol{S}$, and unit outward normal vector, ${}^{r}\boldsymbol{n}$, of the meshing element can be expressed with respect to frame $(xyz)_r$ as follows:

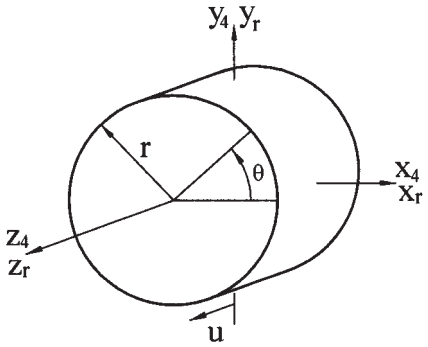

Fig. 3. Conical roller location with respect to translating roller-follower.

$$ {}^{r}\mathbf{S} = [\, rC\theta \quad rS\theta \quad u \quad 1 \,]^{T} \quad \left(-\lambda/2 \le u \le \lambda/2, 0 \le \theta \le 2\pi \right) \tag{5} $$

$$ {}^{r}\mathbf{n} = \frac{\frac{\partial^{r}\mathbf{S}}{\partial u} \times \frac{\partial^{r}\mathbf{S}}{\partial \theta}}{\left\| \frac{\partial^{r}\mathbf{S}}{\partial u} \times \frac{\partial^{r}\mathbf{S}}{\partial \theta} \right\|} = \begin{bmatrix} C\theta \\ S\theta \\ 0 \\ 0 \end{bmatrix}, \tag{6} $$

where θ is the polar angle and λ is the width of the roller.

According to conjugate surface theory [8], the cam profile can be determined from the meshing element as follows:

$$ {}^{0}\mathbf{n}^{T} \bullet \frac{d^{0}\mathbf{S}}{dt} = \left({}^{0}\mathbf{A}_{r}\, {}^{r}\mathbf{n} \right)^{T} \frac{d\left({}^{0}\mathbf{A}_{r}\, {}^{r}\mathbf{S} \right)}{dt} = 0, \tag{7} $$

where ${}^{0}\boldsymbol{S}$ and ${}^{0}\boldsymbol{n}$ are the surface equation. and unit outward normal vector with respect to frame $(xyz)_0$, respectively.

According to Eq. (7), if continuous contact is to be maintained between the roller and the slider cam surface, the relative sliding velocity $d^{0}\mathbf{S}/dt$ (where t is the time variable) must be orthogonal to the common normal ${}^{0}\boldsymbol{n}$ at the contact point. Imposing the condition described in Eq. (7) on Eqs. (5) and (6), the condition of the conjugate points (denoted as $\bar{\theta}$) can be expressed as

$$ \bar{\theta} = -\tan^{-1}\left(\frac{dm}{dt} \Big/ \frac{db_4}{dt} \right), \tag{8} $$

where $\dfrac{dm}{dt} = \left(a_2 S\theta_3 + \dfrac{(a_2 S\theta_3 - e) a_2 C\theta_3}{\sqrt{a_1^2 - (a_2 S\theta_3 - e)^2}} \right) w_3$, and $\dfrac{db_4}{dt} = \dfrac{db_{4a}}{dt}$ is the velocity of the roller-follower and is determined by the motion curve specified for the roller-follower.

The cam profile corresponding to the roller element is obtained by substituting Eq. (8) into Eq. (5), and then transforming ${}^{r}\boldsymbol{S}$ to frame $(xyz)_0$ via the transformation ${}^{0}\boldsymbol{S} = {}^{0}\boldsymbol{A}_{r}\, {}^{r}\boldsymbol{S}$, i.e.

$$^0\mathbf{S} = \begin{bmatrix} ^0S_x & ^0S_y & ^0S_z & 1 \end{bmatrix}^T = \begin{bmatrix} rC\overline{\theta}+m & rS\overline{\theta}+b_4-e & u & 1 \end{bmatrix}^T. \tag{9}$$

Note that the coordinate $^0\boldsymbol{S}_y$ is replaced by $rS\overline{\theta}+b_4$ for reasons of practical convenience. That is, since b_4 and $\overline{\theta}$ are related through Eq. (8), $^0\boldsymbol{S}$ can be expressed solely in terms of u and θ_3 for the given input-output relation $b_4=b_4(\theta_3)$.

3. PRESSURE ANGLE

Having obtained the Eq. of the cam profile, an analytical expression can then be derived for the pressure angle of the slider cam. The pressure angle, ψ, is one of the most important design considerations in the cam-follower mechanism and is defined as the angle between the direction of the unit normal at the cam-roller contact point and the direction of the velocity of the contact point (see Fig. 4) [9]. The pressure angle provides a measure of the efficiency of the force transmission between the cam and the follower. Specifically, the smaller the value of ψ, the better the force transmission. The pressure angle at the contact point p between the slider cam and the roller is given as

$$\tan\psi = \frac{\left\| ^3\mathbf{n}_p \times ^3\mathbf{v}_p \right\|}{\left| ^3\mathbf{n}_p \bullet ^3\mathbf{v}_p \right|}, \tag{10}$$

Where the unit normal vector of the contact point, $^3\mathbf{n}_p$, and the direction of the velocity of the contact point on the roller-follower surface, $^3\boldsymbol{v}_p$, are both defined with respect to frame $(xyz)_3$.

The unit normal vector of the contact point on the roller-follower with respect to frame $(xyz)_3$ is given by

$$^3\mathbf{n}_p = ^3\mathbf{A}_4\,^4\mathbf{A}_r\,^r\mathbf{n}_p = \begin{bmatrix} C\overline{\theta} & 0 & S\overline{\theta} & 0 \end{bmatrix}^T. \tag{11}$$

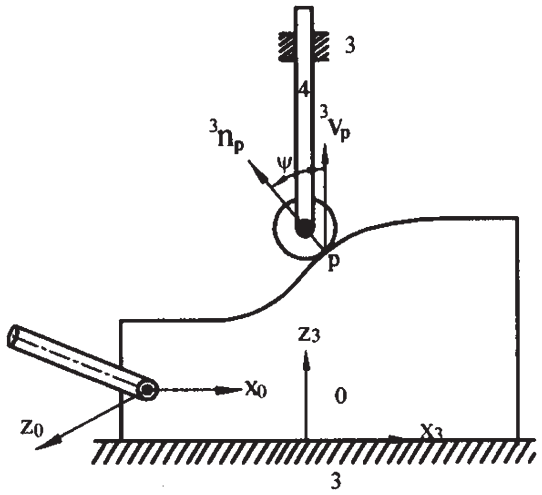

Fig. 4. Pressure angle of slider cam with translating roller-follower.

Meanwhile, the contact point, p, on the roller-follower with respect to frame $(xyz)_3$ is given by

$$ {}^3\mathbf{S}_p = {}^3\mathbf{A}_4\,{}^4\mathbf{A}_r\,{}^r\mathbf{S}_p = {}^3\mathbf{A}_r\,{}^r\mathbf{S}_p = \begin{bmatrix} 1 & 0 & 0 & 0 \\ 0 & 0 & -1 & 0 \\ 0 & 1 & 0 & b_4 \\ 0 & 0 & 0 & 1 \end{bmatrix} \begin{bmatrix} rC\overline{\theta} \\ rS\overline{\theta} \\ u \\ 1 \end{bmatrix} = \begin{bmatrix} rC\overline{\theta} \\ -u \\ rS\overline{\theta} + b_4 \\ 1 \end{bmatrix}. \tag{12} $$

Since the translating roller-follower translates along the z_3 axis, the direction of the velocity of the contact point on the roller-follower surface with respect to frame $(xyz)_3$ can be obtained as

$$ {}^3\mathbf{v}_p = \frac{d^3S}{dt} = \begin{bmatrix} 0 & 0 & \dfrac{db_4}{dt} & 0 \end{bmatrix}^T. \tag{13} $$

Using the inner product, the pressure angle, ψ, can be derived as

$$ \tan\psi = \left|\cot\overline{\theta}\right|. \tag{14} $$

4. ANALYSIS OF CURVATURE

When machining the slider cam, undercutting occurs if the radius of the cutting tool is greater than the minimum absolute value of the radius of curvature of the cam. Similarly, in the roller-follower mechanism, interference between the roller and the slider cam profile occurs if the minimum absolute value of the radius of curvature of the cam is less than the roller radius. Therefore, the principal curvatures of the slider cam surface must be carefully analyzed and designed in order to prevent the occurrence of singular points and to generate a geometrically feasible mechanism.

In accordance with the principles of differential geometry, the principal curvatures of the cam surface can be evaluated from the derived mathematical model of the slider cam, ${}^0\mathbf{S}(\theta_3,u)$, as follows:

$$ K_1, K_2 = H \pm \sqrt{H^2 - K}, \tag{15} $$

Where K_1 and K_2 are the principal curvatures, and H and K are defined as

$$ H = \frac{2FM - EN - GL}{2(EG - F^2)}, K = \frac{LN - M^2}{EG - F^2} \tag{16} $$

where $L = {}^0n \bullet \dfrac{\partial^{20}S}{\partial^2 u}$, $M = {}^0n \bullet \dfrac{\partial^{20}S}{\partial u \partial\theta_3}$, $N = {}^0n \bullet \dfrac{\partial^{20}S}{\partial^2\theta_3}$, $E = \dfrac{\partial^0 S}{\partial u} \bullet \dfrac{\partial^0 S}{\partial u}$, $F = \dfrac{\partial^0 S}{\partial u} \bullet \dfrac{\partial^0 S}{\partial\theta_3}$ and $G = \dfrac{\partial^0 S}{\partial\theta_3} \bullet \dfrac{\partial^0 S}{\partial\theta_3}$ (see (A1~A6) in Appendix A).

From Eqs. (15) and (16), it can be seen that the principal curvatures of the slider cam are related to both the roller-follower motion program and the dimensions of the kinematic model of the slider-crank.

5. ANALYSIS OF KINEMATIC PERFORMANE

Before the slider cam profile can be designed, it is first necessary to specify a suitable motion curve for the roller-follower such that the dynamic loading effects are minimized. In this paper, it is assumed that the displacement of the roller-follower is governed by the modified sine curve shown in Fig. 5, in which b_{4a} is the roller-follower displacement in the vertical direction, θ_3 is the crank rotational angle, and θ_d is the dwell period. As shown, the modified sine curve starts from the zero position and designates the total rise of the roller-follower during the period of one crank rotation as h during the period of the crank rotation, τ. The equations of displacement, b_{4a}, for the modified sine curve [10] are given as follows:

$$b_{4a}(\theta_3)=\begin{cases} h\left[\dfrac{\pi}{4+\pi}\dfrac{\theta_3-\theta_d}{\tau}-\dfrac{1}{4(4+\pi)}S\left[4\pi\dfrac{\theta_3-\theta_d}{\tau}\right]\right], 0\le\theta_3-\theta_d\le\dfrac{\tau}{8} \\ h\left[\dfrac{2}{4+\pi}+\dfrac{\pi}{4+\pi}\dfrac{\theta_3-\theta_d}{\tau}-\dfrac{9}{4(4+\pi)}S\left(\dfrac{4\pi}{3}\dfrac{\theta_3-\theta_d}{\tau}+\dfrac{\pi}{3}\right)\right], \dfrac{\tau}{8}\le\theta_3-\theta_d\le\dfrac{7\tau}{8} \\ h\left[\dfrac{4}{4+\pi}+\dfrac{\pi}{4+\pi}\dfrac{\theta_3-\theta_d}{\tau}-\dfrac{1}{4(4+\pi)}S\left(4\pi\dfrac{\theta_3-\theta_d}{\tau}\right)\right], \dfrac{7\tau}{8}\le\theta_3-\theta_d\le\tau \end{cases} \quad (17)$$

Since the slider cam moves back and forth as the input crank rotates through 360^0, for each specified slider cam position, there exists two corresponding crank angles, as shown in Fig. 6. The forward and backward strokes of the slider cam are a complementary response to a full cycle of the input crank, but share a common slider cam profile. Therefore, the complete roller-follower motion is described by a double-dwell curve. However, in practice, the roller-follower motion can be analyzed by arbitrarily choosing either the forward stroke or the backward stroke of the slider cam.

Since the roller-follower motion has the form of a double-dwell curve, it is necessary to consider six specific positions of the crank rotational angle, i.e. (p_1,..p_6) (see Fig. 6). Of these six positions, positions p_1 and p_4 are of particular interest since they correspond to the two limiting positions of the slider-cam. From Fig. 6, positions p_1 and p_4 can be obtained as

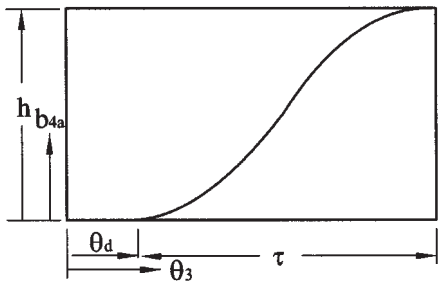

Fig. 5. Modified sine motion curve.

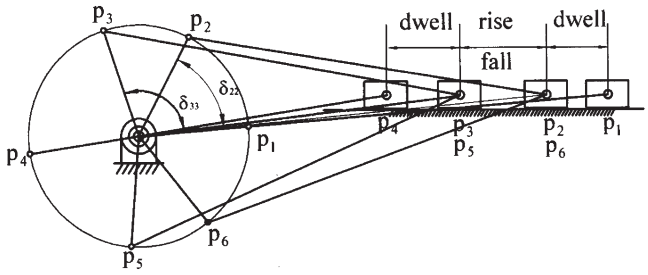

Fig. 6. Six segments of roller-follower motion.

$$p_1 = Sin^{-1}\left(\frac{e}{a_1 + a_2}\right), \tag{18}$$

$$p_4 = Sin^{-1}\left(\frac{e}{a_1 - a_2}\right) + \pi. \tag{19}$$

Parameter p_2 is a design value designated for θ_3. The slider cam position, s, corresponding to θ_3 is given by

$$s = a_2 C\theta_3 + \sqrt{a_1^2 - (a_2 S\theta_3 - e)^2}. \tag{20}$$

Applying the cosine law, δ_{22} is obtained as

$$\delta_{22} = Cos^{-1}\left(\frac{a_2^2 + (s^2 + e^2) - a_1^2}{2a_2\sqrt{s^2 + e^2}}\right). \tag{21}$$

Thus, the crank angle position p_6 can be expressed as

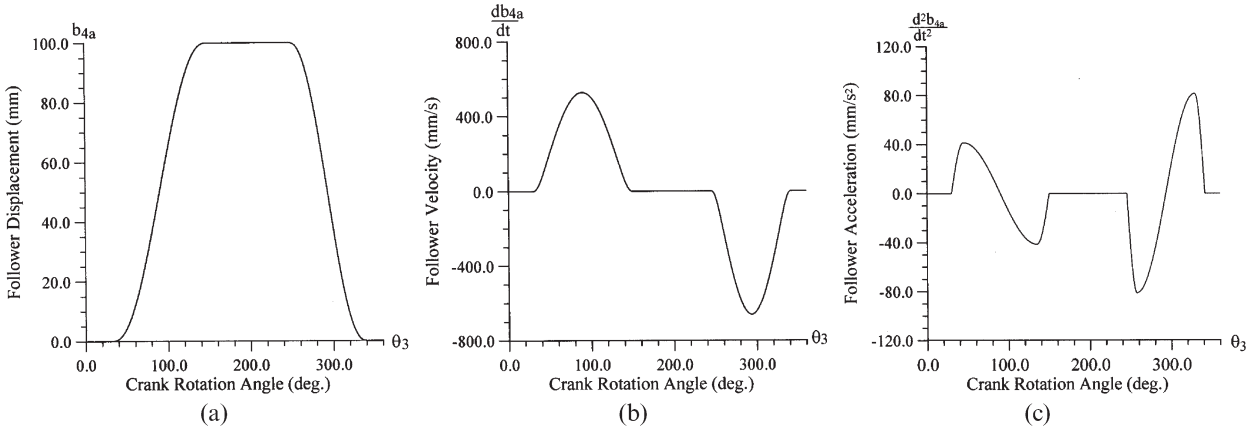

Fig. 7. Kinematic analysis of translating roller-follower: (a) displacement diagram; (b) velocity diagram; (c) acceleration diagram.

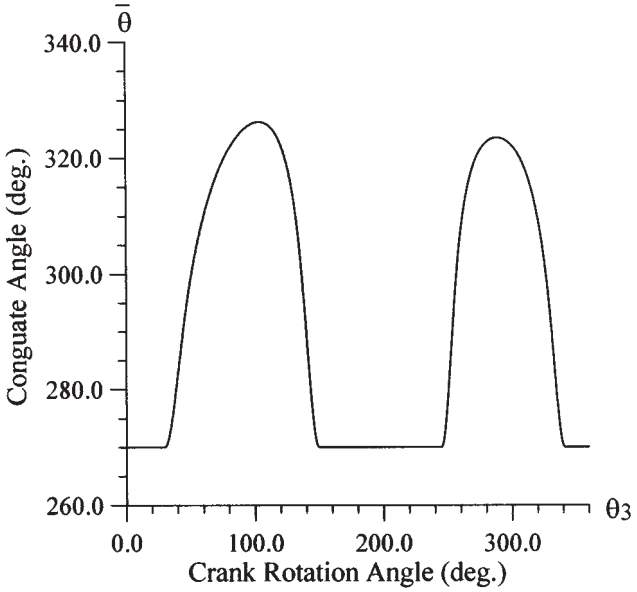

Fig. 8. Variation of conjugate angle for translating roller-follower.

$$p_6 = p_2 + 2\pi - 2\delta_{22} \tag{22}$$

Similarly, the design parameter p_3 is designated for θ_3 and the corresponding position of the slider cam, s, can be obtained by substituting θ_3 into Eq.(20). Applying the cosine law yields

$$\delta_{33} = Cos^{-1}\left(\frac{a_2^2 + (s^2 + e^2) - a_1^2}{2a_2\sqrt{s^2 + e^2}}\right). \tag{23}$$

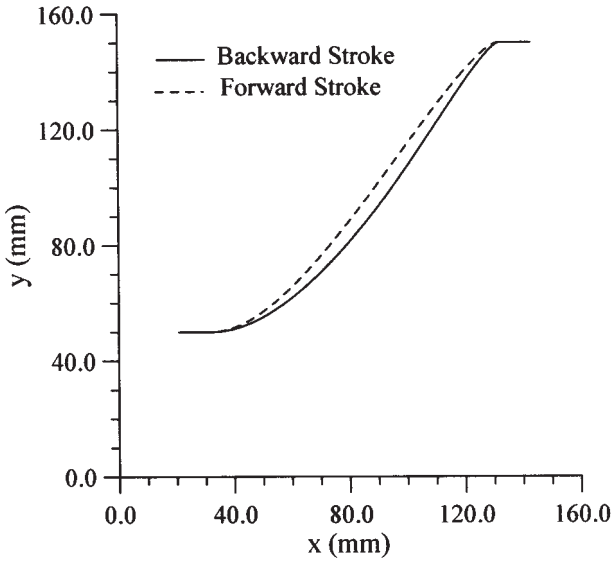

Fig. 9. Simulated profiles of slider cam.

Thus, the crank angle position p_5 can be obtained as

$$p_5 = p_3 + 2\pi - 2\delta_{33} \tag{24}$$

In the forward stroke of the slider cam, the active period is defined as $\tau = p_3 - p_2$ and the dwell period is given by $\theta_d = p_2$. Conversely, in the backward stroke, the active period is given by $\tau = p_5 - p_6$ while the dwell period is defined as $\theta_d = p_5$. Therefore, the reciprocating motion of the offset slider-crank yields an asymmetrical displacement of the roller-follower.

For illustration purposes, this study considers the case of an offset slider-crank and translating roller-follower mechanism with the following parameters: $a_1 = 100$ mm, $a_2 = 60$ mm, $a_3 = 180$ mm, $e = 15$ mm, $b_{40} = 58$ mm, $p_2 = 30^0$, $p_3 = 150^0$ and $h = 100$ mm, respectively. Combining Eq. (17) with Eqs. (18) and (24), rotational crank positions p_1, p_4, p_5 and p_6 are obtained as $p_1 = 5.379^0$, $p_4 = 202.024^0$, $p_5 = 245.467^0$ and $p_6 = 341.359^0$, respectively. Figure 7 shows the corresponding kinematic characteristics of the translating roller-follower for an assumed crank angular velocity of 60 rpm and a roller radius of 8 mm. The variation in the conjugate angle of the translating roller-follower can be derived from Eq. (8) and has the form shown in Fig. 8. Meanwhile, the simulated profile of the designed slider cam can be obtained from Eq. (9) and is shown in Fig. 9. Finally, the variation in the principal curvature of the designed slider cam has the form shown in Fig. 10.

Once the distance between the main shaft and the translating follower has been determined, i.e. a_3, the remaining design parameters can also be derived, namely the link length, the active period, the total rise and the offset. To examine the variation in the pressure angle of the slider-crank, Table 2 presents four illustrative sets of design parameters. Note that to isolate the kinematic effects of the major design parameters, one parameter in each design set is deliberately assigned a value different from that assigned in the remaining sets. Figure 11 presents the pressure angle plots computed using Eq. (14) for the four parameter design sets. Comparing the four figures, it can be seen that the pressure angle is determined primarily by the total rise parameter h, but is also strongly affected by parameters p_2 and p_3, i.e. the active

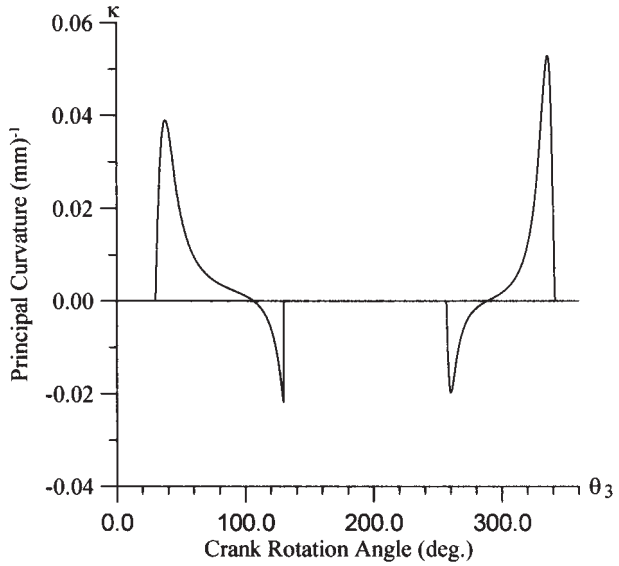

Fig. 10. Variation of principal curvature of designed slider cam.

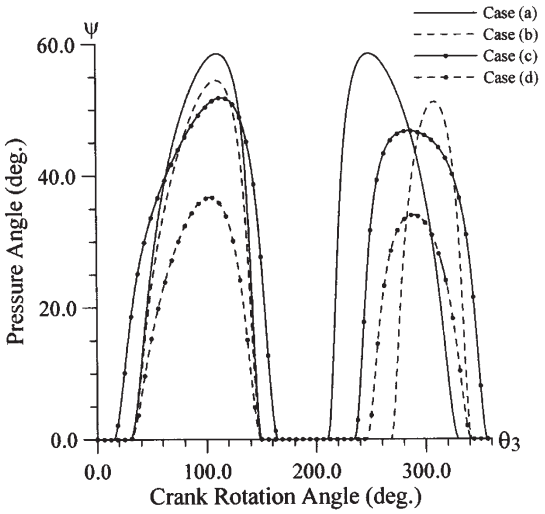

Fig. 11. Pressure angle plots for four design cases shown in Table 2.

period. Since the pressure angle produces a significant instantaneous force–transmission effect during crank rotation, the results presented in Fig. 11 suggest that given a constraint on the maximum permissible rise, h, the active period defined by crank rotation points p_2 and p_3 should be increased. To further investigate the effects of design parameters a_1, a_2 and e on the pressure angle, Table 3 presents an additional three sets of design parameters. The corresponding pressure angle plots are presented in Fig. 12(a), while the slider cam displacements are shown in Fig. 12(b). Comparing the two figures, it can be seen that the magnitude of the pressure angle reduces as the stroke of the slider cam increases.

6. CUTTER TOOL PATH

In generating the NC data required to machine the slider cam in the mechanism shown in Fig. 2, it is first necessary to determine the desired cutter location (the position and orientation of the cutter) with respect to the slider cam frame $(xyz)_0$. Figure 13 illustrates the position of the cylindrical end miller with respect to the roller-follower at the kth cut. The configuration of the cutting tool relative to the roller frame is expressed as

$$ {}^{r}\mathrm{A}_t = \begin{bmatrix} ? & ? & 0 & f \\ ? & ? & 0 & 0 \\ ? & ? & -1 & \lambda/2 - kd \\ 0 & 0 & 0 & 1 \end{bmatrix}, \tag{25} $$

Table 1. Kinematic parameters of slider crank mechanism with meshing translating roller-followers.

link	b_i	θ_i	a_i	α_i
1	0	θ_1	a_1	0^0
2	0	$-\theta_2$	$-a_2$	0^0
3	0	$-\theta_3$	a_3	-90^0
4	b_4	0	0	90^0

Table 2. Design parameters for numerical examples in Fig. 11.

	a_1	a_2	p_2	p_3	h	e
Case (a)	100	60	30^0	150^0	100	0
Case (b)	90	70	30^0	150^0	100	15
Case (c)	100	60	15^0	165^0	100	15
Case (d)	100	60	30^0	150^0	50	15

where $w=kd$ (d is the allowable cutting depth) and f define the current cutting position. Note that the third column in Eq. (25) indicates the desired orientation of the cutter axis. Since the cylindrical end miller is a rotational cutting tool, its x_t and y_t orientations are of no interest.

Combining Eq. (4) and Eq. (25), the desired cutter location with respect to frame $(xyz)_0$ is given by

$$ {}^0\mathrm{A}_t = {}^0\mathrm{A}_r\,{}^r\mathrm{A}_t = \begin{bmatrix} ? & ? & 0 & f+m \\ ? & ? & 0 & b_4-e \\ ? & ? & -1 & \lambda/2-kd \\ 0 & 0 & 0 & 1 \end{bmatrix}. \tag{26} $$

Figure 14 presents a schematic illustration of the 3-axis machining center used in the present study. To determine the NC data commands required to machine the cam, it is first necessary to number the links of the machining center sequentially, beginning with the clamping system (designated as "$\underline{0}$") and ending with the spindle link (designated as "$\underline{3}$"). Once the frames ${}^{\underline{i-1}}\underline{A}_{\underline{i}}$ ($i=\underline{1},\underline{2},\underline{3}$) have been assigned according to the D–H notation, the various link parameters can be tabulated, as shown in Table 4. Note that $\underline{b}_1$, $\underline{b}_2$ and $\underline{b}_3$ are link variables which control the movements of the machine components. The cutter location matrix with respect to the blank frame $(xyz)_0$ can be expressed as

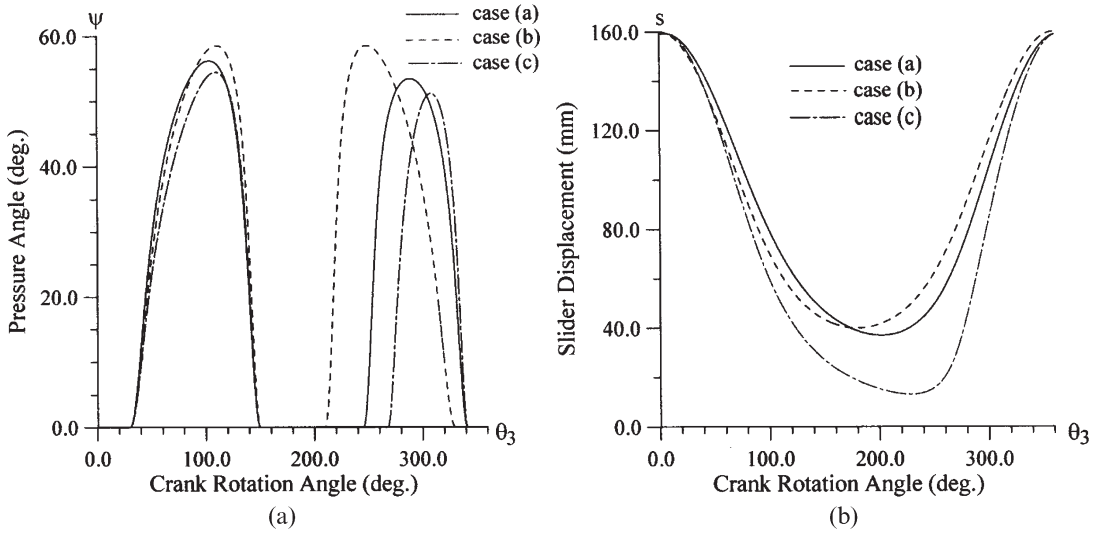

Fig. 12. (a) Pressure angle plots and (b) slider displacement plots for three design cases shown in Table 3.

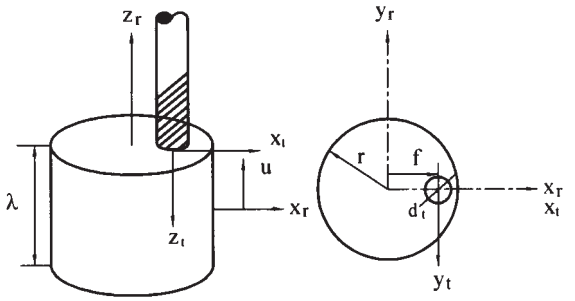

Fig. 13. Milling cutter location with respect to meshing element.

$$ {}^{0}\underline{\mathrm{A}}_{t} = \begin{bmatrix} ? & ? & 0 & -\underline{b}_1 \\ ? & ? & 0 & -(\underline{a}_3 + \underline{b}_2) \\ ? & ? & -1 & \underline{a}_1 - \underline{b}_3 - \underline{d} \\ 0 & 0 & 0 & 1 \end{bmatrix}. \tag{27} $$

(Note that the derivation of Eq. (27) is fully described in [11]). Eq. (27) describes the configuration of the 3-axis machining center with respect to the slider cam blank.

Referring to Fig. 14, the desired NC position commands for the X-, Y-, and Z-axes of the 3-axis machine relative to the slider cam blank frame $(xyz)_0$ can be expressed as

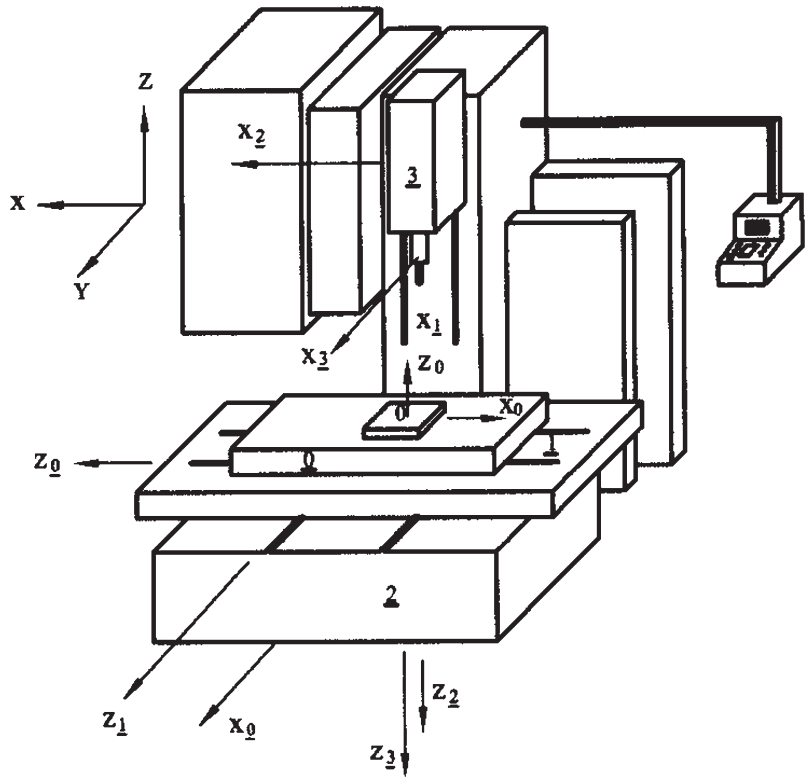

Fig. 14. 3-axis vertical machine tool.

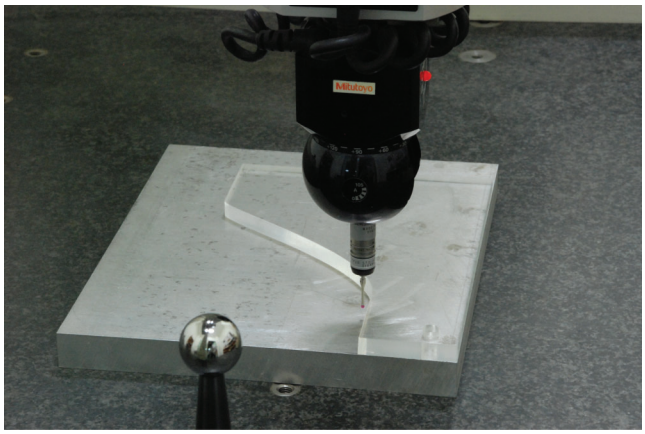

Fig. 15. Measurement of the machined slider cam on 3-axis CMM.

$$X = f + m, \tag{28}$$

$$Y = b_4 - e, \tag{29}$$

$$Z = (\lambda/2) - k\,d. \tag{30}$$

In order to verify the methodology developed in this study, a slider-crank and translating roller-follower mechanism with the following parameters was designed: $a_1=100$ mm, $a_2=60$ mm, $a_3=180$ mm, $e=15$ mm, $h=100$ mm, $b_{40}=58$ mm, $p_2=30^0$, $p_3=150^0$, $\lambda=10$ mm and $r=8$ mm. The input-output relationship was defined in accordance with the modified sine motion curve shown in Fig. 5 and the machined slider cam was based on the backward stroke. The analytical results for the principal curvatures of the slider cam revealed that no undercutting took place between the cam surface and the cutting tool or roller (i.e. the minimum radius of curvature of the cam profile was determined to be 25.707 mm while the cylindrical end miller had a radius of 8 mm). The machined slider cam (shown in Fig. 15) was inspected using a coordinate measuring machine (Mitutoyo BHN-710) [12]. Note that the hole is considered as the reference point of the machined workpiece. i.e. the offset point of the slider cam. Table 5 compares the measured coordinates with the design coordinates at designated positions on the cam surface. The results indicate that the maximum deviation of the machined surface from the design profile is 20 μm. A satisfactory agreement was found between the measured dimensions and the design profile,

Table 3. Design parameters for numerical examples in Fig. 12.

	a_1	a_2	p_2	p_3	h	e
Case (a)	100	60	30^0	150^0	100	15
Case (b)	100	60	30^0	150^0	100	0
Case (c)	90	70	30^0	150^0	100	15

Table 4. Kinematic parameters of the 3-axis milling machine.

link	$\underline{b}_i$	$\underline{\theta}_i$	$\underline{a}_i$	$\underline{\alpha}_i$
1	$\underline{b}_1$	90^0	$\underline{a}_1$	90^0
2	$\underline{b}_2$	90^0	0	-90^0
3	$\underline{b}_3$	-90^0	$\underline{a}_3$	0^0

thus confirming the ability of the proposed methodology to provide a satisfactory description of the offset slider-crank mechanism with a translating roller-follower.

7. CONCLUSION

This paper has used a homogenous coordinate transformation method to develop a generic mathematical model of an offset slider-crank mechanism with a translating roller-follower. Given the fundamental design parameters, the proposed methodology not only determines the pressure angle and principal curvature of the slider cam, but also generates the NC data required for machining purposes. Moreover, the mathematical model enables the kinematic characteristics of the designed mechanism to be systematically explored. Overall, the methodology presented in this study provides an effective approach for the design and analysis

Table 5. Comparison of designed and measured coordinates at designated points on cam surface.

Designed coordinates		Measured coordinates	
x_i (mm)	y_i (mm)	x_i (mm)	y_i (mm)
20.705	50	20.706	49.995
22.105	50	22.106	49.994
26.183	50	26.184	49.996
33.145	50.091	33.145	50.085
43.942	52.403	43.938	52.406
55.591	58.604	55.584	58.598
67.451	68.17	67.442	68.185
79.276	80.433	79.280	80.434
90.672	94.465	90.673	94.478
101.253	109.104	101.249	109.110
110.719	123.076	110.711	123.088
118.874	135.120	118.872	135.126
125.545	144.094	125.545	144.104
130.267	149.016	130.255	149.024
131.813	149.947	131.811	149.961
134.163	150	134.164	150.020
137.325	150	137.326	150.014
139.75	150	139.751	150.010
141.487	150	141.488	150.010
142.551	150	142.552	150.011
142.919	150	142.920	150.011

of offset slider-cranks with translating roller-followers, and facilitates their manufacture in an automatic and controllable manner.

REFERENCES

1. Wu, Long-Iong, Chang, Wen-Tung and Liu, Chun-Hsien, "The design of vary-velocity translating cam mechanisms," *Mechanism and Machine Theory,* Vol. 42, pp. 352–364, 2007.
2. Shigly, J.E. and Uicker, J.Jr., *Theory of Machines and Mechanisms,* McGraw-Hill, New York, 1995.
3. Ghosh, A. and Yadav, R.P., "Synthesis of cam-follower systems with rolling contact," *Mechanism and Machine Theory*, Vol. 18, pp. 49–56, 1983.
4. Tsay, D.M. and Hsien, M.W., "Design and machining of cylindrical cams with translating conical followers," *Journal of Computer-Aided Design*, Vol. 25, pp. 655–661, 1993.
5. Tsay, D.M. and Hsien, M.W., "A general approach to the determination of planar and spatial cam profiles," *ASME Journal of Mechanical Design*, Vol. 118, pp. 259–265, 1996.
6. DasGupta, Anirvan and Ghosh, Amitabha, "On the determination of basic dimensions of a cam with a translating roller-follower," *ASME Journal of Mechanical Design*, Vol. 126, pp. 143–147, 2004.
7. Paul, R.P., *Robot Manipulators-Mathematics, Programming and Control,* MIT press, Cambridge, Mass 1982.
8. Chakraborty, J. and Dhande, S.G., *Kinematics and Geometry of Planar and Spatial Cam Mechanisms,* John Wiley & Sons, New York, 1977.
9. Gonzalez-Palacios, M. A. and Angeles, J., *Cam Synthesis,* Kluwer Academic Publisher, 1993.
10. Jensen, Preben W., *Cam design and manufacture,* Marecl Dekker, Inc., 1987.
11. Hsieh, J.-F., **"**Application of homogenous transformation matrix to the design and machining of a geneva mechanism with curved slots," *Proc. Instn. Mech. Engrs, Part C: J. Mechanical Engineering Science,* Vol. 221 pp. 1435–1443, 2007.
12. Hsieh, J.-F. and Lin, P. D., "Application of homogenous transformation matrix to measurement of cam profiles on coordinate measuring machines," *Journal of Machine Tools & Manufacture*, Vol. 47, pp. 1593–1606, 2007.

APPENDIX A

The principal curvature of the slider surface can be evaluated by Eqs. (15) and (16), and their related parameters have been derived as the following:

$$L = 0 \tag{A1}$$

$$M = 0 \tag{A2}$$

$$N = \frac{d^2 b_4}{d\theta_3^2} S\overline{\theta} + \left[a_2 C\theta_3 + \frac{(a_2 S\theta_3 - e)^2 a_2^2 C^2\theta_3}{\left[a_1^2 - (a_2 S\theta_3 - e)^2\right]^{\frac{3}{2}}} + \frac{a_2^2 C^2\theta_3 - a_2^2 S^2\theta_3 + a_2 e S\theta_3}{\sqrt{a_1^2 - (a_2 S\theta_3 - e)^2}} \right] C\overline{\theta} - r\left(\frac{d\overline{\theta}}{d\theta_3}\right)^2 \tag{A3}$$

$$E = 1 \tag{A4}$$

$$F = 1 \tag{A5}$$

$$G = \left(\frac{db_4}{d\theta_3}\right)^2 + \left[a_2 S\theta_3 + \frac{(a_2 S\theta_3 - e) a_2 C\theta_3}{\sqrt{a_1^2 - (a_2 S\theta_3 - e)^2}} \right]^2 + 2\left[\left(a_2 S\theta_3 + \frac{(a_2 S\theta_3 - e) a_2 C\theta_3}{\sqrt{a_1^2 - (a_2 S\theta_3 - e)^2}} \right) C\overline{\theta} - \left(\frac{db_4}{d\theta_3}\right) S\overline{\theta} \right] r\frac{d\overline{\theta}}{d\theta_3} + r^2\left(\frac{d\overline{\theta}}{d\theta_3}\right)^2 \tag{A6}$$